Excited-state absorption spectroscopy of self-trapped excitons in alkali halides

R. T. Williams and M. N. Kabler
Naval Research Laboratory, Washington, D.C. 20375
(Received 30 August 1973)

Optical transitions between the lowest metastable triplet state and higher states of the self-trapped exciton are reported for nine alkali halides, in the energy range from 0.6 to 5.5 eV. Measurements were made on pure crystals using techniques of time-resolved spectroscopy and electron-pulse irradiation. Variation of the transition energies with lattice constant provides additional evidence for the classification of the spectra in terms of two basic categories: hole transitions localized on the X_2^- core, and electron transitions largely decoupled from the influence of the core ions. Optical binding energies of the self-trapped exciton are estimated from the spectra, and are found to be 2–4 times greater than the binding energies of corresponding unrelaxed excitons. The relaxation of the lattice around the exciton is discussed in terms of a two-dimensional configuration-coordinate model. Hole self-trapping and the Stokes shift of emission occur principally through the axial mode, as commonly accepted. The increase of exciton binding energy upon relaxation to the equilibrium configuration is attributed to a nonaxial mode of relaxation which may be viewed as analogous to the breathing mode that broadens and shifts M-center transitions.

INTRODUCTION

The low-lying states of self-trapped excitons (STE's) in alkali halide crystals have been studied extensively by means of the luminescence emitted during electron-hole recombination. These investigations have shown that the metastable self-trapped configuration in which the luminescence originates consists of an electron bound to a hole which is itself localized on a pair of nearest-neighbor halide ions. The hole configuration is equivalent to the well-known stable X_2^- or V_k center.[1,2] The recombination luminescence spectra consist of broad bands, some of which are σ polarized, short-lived, and due to the decay of singlet excited states, and others which are π polarized, relatively long-lived, and due to triplet states.[3] The present article concerns the use of time-resolved optical-absorption spectroscopy to observe transitions from the lowest metastable triplet state to higher triplet states of the STE.

The first results of these studies, dealing mainly with NaCl, KCl, and RbCl, were reported in an earlier letter.[4] A subsequent communication described new transient absorption bands observed in alkali iodides in the ultraviolet spectral region and identified them as fundamental crystal (exciton) transitions perturbed by the presence of triplet STE's.[5]

These investigations have now been extended to include nine alkali halides. The results remain generally consistent with the earlier conclusions concerning the nature of the higher STE triplet states. In addition, we are able to expand somewhat our initial arguments regarding the origin of the relatively large optical binding energies obtained for the electron and hole in the lowest STE triplet state.

The present data are in essential agreement with the more recent transient-absorption results of Hirai *et al.*,[6] for KCl and NaCl and Kondo *et al.*,[7] for KBr, although there are differences in detail. The Sendai group has emphasized F- and H-center production by pulsed radiation, whereas the work described here deals primarily with the triplet STE.

THE EXPERIMENT

A schematic diagram of the equipment we employed to make time-resolved measurements of absorption and emission is shown in Fig. 1.[8] The radiation source was a small commercial electron accelerator which operates by capacitor discharge to produce a 5-nsec electron pulse of up to 10 J total energy. The mean electron energy in the pulse was about 500 keV. The penetration depth for electrons of this energy in a typical alkali halide is only of the order of 0.5 mm. Therefore, to obtain an easily measurable optical density from this thin layer of coloration, the monitoring light beam was internally reflected at a low angle from the target face of the crystal, as shown in Fig. 1. Optical path lengths up to 10 times the thickness of the irradiated portion were obtained in this way. Samples (typically $1.5\times1.5\times0.3$ cm) were cleaved from single crystals and were mounted on the cold finger of a standard optical Dewar with a 0.025-mm-thick titanium window for the electron beam. A variable-temperature helium Dewar with a germanium resistance thermometer on the cold finger was used when measurements over a range of temperatures were required. Determinations of the electron-pulse energy were made by substituting silver-activated glass-block dosimeters for the samples. The energy density per electron pulse ranged from about 10^{16} to 10^{17} eV/cm^2 at the sample surface in

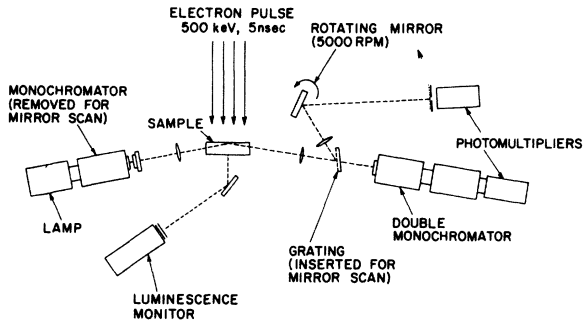

FIG. 1. Schematic diagram of the apparatus. Two alternative methods of optical detection are shown.

this experiment. Some sample heating effects were observed at high pulse energies, but these could usually be reduced to negligible proportions by reducing the beam energy.

Several optical detection systems were used interchangeably, depending on the particular sample and the parameter to be measured. Decay times at a single wavelength were measured by means of the double monochromator and photomultiplier in the lower right of Fig. 1, yielding a display of light intensity versus time on an oscilloscope. A dc lamp with a shutter was used to monitor long-lived ($\tau > 10^{-3}$ sec) absorption bands. A xenon flash lamp was used when working with shorter-lived bands, primarily in order to discriminate against the luminescence. The peak power of the luminescence becomes quite high under the conditions of this experiment; for NaI, the extreme case, the emission over 4π sr can exceed 1 kW.

Low-resolution spectra could be obtained by a succession of fixed-wavelength measurements, but because of fluctuations in electron-pulse energy and beam focus it was necessary to normalize the dose received at the sample surface by simultaneously monitoring luminescence. For crystals with a high efficiency of permanent coloration, the multiple shots required to obtain a spectrum in this way were a disadvantage. Better resolution of detail in relatively long-lived absorption spectra was obtained by inserting the grating (or prism) indicated in Fig. 1. A rotating mirror deflected the imaged spectrum across the photomultiplier slit in synchronization with the electron pulse and lamp flash. The time axis of the oscilloscope display was then proportional to wavelength, so that a spectrum could be recorded with each revolution of the mirror. Wavelength scanning rates of up to 60 Å/μsec were achieved. Calibration by narrow-line discharge lamps resulted in spectra which, though rather crude by usual spectroscopic standards, were adequate for the broad bands investigated. The data obtained in this way were useful, for example, in refining measurements of the doublet structure in the infrared bands of RbBr, KBr, and KCl, to be discussed presently. Spectra obtained by high-speed scanning were in all cases checked against fixed wavelength data. The interpretation of spectra obtained by this photoelectric method was inherently simpler than the interpretation of photographic data, which were occasionally used. The scanning method was, of course, limited to the study of bands whose decay times were long compared to the scan time. Small corrections for decay during a scan were made when required.

Repetitive excitation and a digital signal averager were used when the signal-to-noise ratio was low, or when it was desired to reduce the electron pulse energy to avoid transient heating effects. Infrared measurements beyond 1.1 μm were made using a cooled InSb detector with a 2-μsec time constant. Shorter wavelengths were covered by various photomultiplier tubes. Within the time constraints noted, the over-all apparatus was capable of measuring absorption spectra throughout the wavelength range 0.21–2.5 μm.

EXPERIMENTAL RESULTS

Figures 2–4 present the time-resolved optical-absorption spectra for nine alkali-halide crystals. The measurements were made at a temperature of 9 ± 3 K. The decay-time components which constitute each spectrum have been separated in the figures and are listed in the respective figure keys. The use of the symbols (=) and ($\approx$) in the figure keys is intended to distinguish strictly exponential decay processes for which τ is the $1/e$ time from those which can only be characterized by an approximate time τ for decay.

Each curve, solid or broken, represents the initial value of one component in the decay time analysis of optical absorption. The analysis will be illustrated later for the cases of RbI and RbBr. The solid-line spectra in Figs. 2–4 represent those components of absorption which share the time dependence of the principal triplet-exciton emission band in each respective material. The broken curves show other components, most notably some small, stable color-center bands and intense, rapidly decaying bands, which are also identified with color centers. The sum of all component spectra shown for a given material is the total absorption immediately following the pulse. "Immediately," as used here, has not been defined precisely by rise-time measurements, but our own observations and those of Karasawa and Hirai[9] and Kondo *et al.*,[7] indicate that the growth of the absorption is in most cases no slower than the 5-nsec electron pulse width.[10]

The points shown are those from which the solid curves were determined; i.e. they are the extrap-

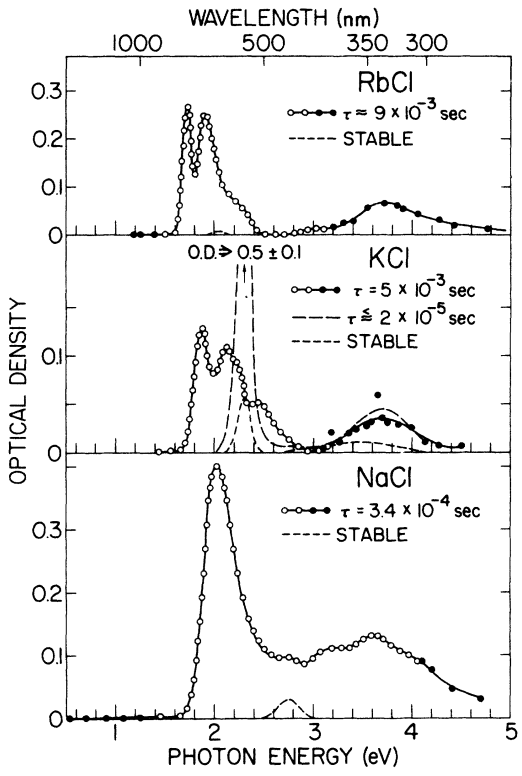

FIG. 2. Time-resolved spectra of optical absorption induced in samples at 9±3 K by a pulse of 500-keV electrons. The spectra shown in solid lines with experimental points share the decay time of the emission from the lowest triplet state of the self-trapped exciton, and are attributed to excited-state transitions originating in that state. Solid data points were measured point-by-point, while open points are representative of continuous-wavelength data obtained by high-speed scan.

olated zero-time components of absorption which can be correlated with the STE decay time. The broken curves were determined by similar points resulting from analysis of the same data, but those points have been left out of the figures for clarity. Filled circles show data which were taken at one fixed wavelength per electron pulse, while the open circles are representative data points obtained by the rapid-scanning method described earlier. All parts of the spectra shown have been covered at least by the fixed-wavelength method, which is the basis for decay-time assignments. However some of the detailed spectral features at low energies were resolved much better in the rapid-scan data, and we have chosen to display those scan points where appropriate to convey our best obtainable resolution in spectral shape.

Verification that two spectral components share the same lifetime was limited by uncertainty in both the experiment and in the decay-time analysis, which in turn varied for different parts of the spectrum. One example of fairly uncomplicated decay-time assignments is the case of RbI, shown in Fig. 5. The time development of each of the major spectral features, including the 2.3-eV luminescence, is plotted on a semilogarithmic scale, and straight lines parallel to the luminescence decay line are drawn through the data. The 5.61-eV absorption data show more scatter because of shot noise in the transmitted light beam, which has a lower intensity at this energy. On the other hand, the expected error at 1.2 eV is quite small, so that a small fast-decaying component may be readily distinguished from the major component which clearly shares the luminescence decay time. Components of stable absorption too small to be shown in Fig. 4 (≈2%) were detected at the *F*-band energy and near 2.8 eV, and were subtracted from the 1.75- and 2.82-eV decay curves.

The precision to which decay times have been measured for all spectral components in NaCl,

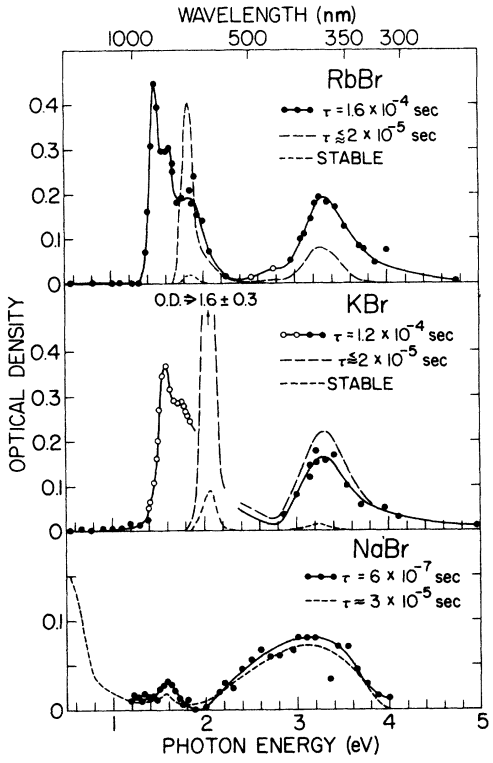

FIG. 3. Time-resolved spectra of optical absorption induced in samples at 9±3 K by a pulse of 500-keV electrons. The spectra shown in solid lines with experimental points share the decay time of the emission from the lowest triplet state of the self-trapped exciton, and are attributed to excited-state transitions originating in that state. Solid data points were measured point-by-point, while open points are representative of continuous-wavelength data obtained by high-speed scan.

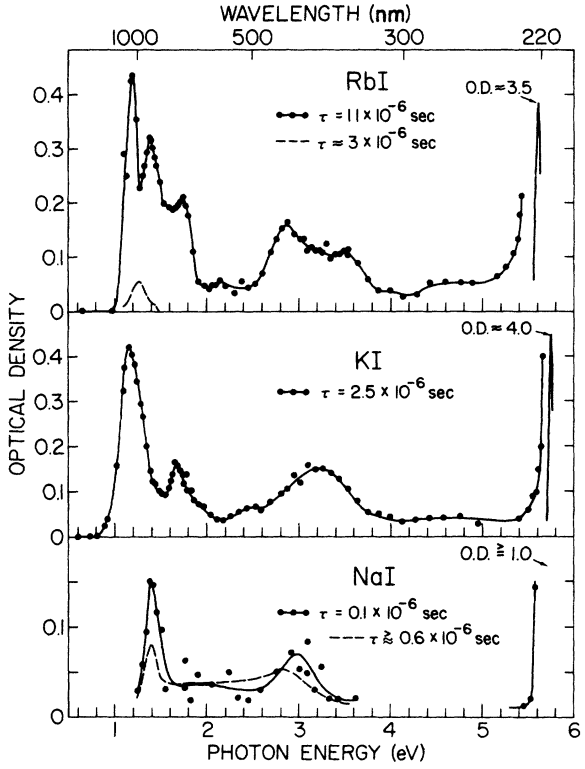

FIG. 4. Time-resolved spectra of optical absorption induced in samples at 9±3 K by a pulse of 500-keV electrons. The spectra shown in solid lines with experimental points share the decay time of the emission from the lowest triplet state of the self-trapped exciton, and are attributed to excited-state transitions originating in that state.

RbCl, and KI is comparable to the example of RbI; that is, 10% or better. The same precision applies to the infrared bands in all crystals, since they are not overlapped by any other strong components. In Fig. 6, RbBr serves as an example of a crystal with substantial overlapping decay-time components, which we identify as transient *F* and *H* bands and a stable *F* band. Because of the uncertainties involved in making a three-part decomposition of the decay curve, the expected error *for wavelengths in the F-band* is on the order of 25% for RbBr. The expected error in the *F*-band is higher for KBr because of the larger *F* band, but is lower for KCl because of the greater difference in decay times of the *F* and STE.

In the case of NaI, we observe two decay-time components in absorption, and two corresponding components in the 4.2-eV luminescence. The limit of agreement is on the order of 20%, and there is some indication that the longer decay time depends on the treatment of the sample and/or the temperature. Similar luminescence components of lifetimes 0.11[11] and 0.57 μsec[12] have been noted by other investigators. The ratio of integrated intensities of the two luminescence components measured at 4.2 eV is roughly consistent with the relative strengths of the absorption components. In view of the comparability of the absorption spectra for the two components (Fig. 4), it is probable that both are associated with the self-trapped exciton.

In NaBr we again find two components of absorption, 0.6 and 30 μsec, with roughly the same strength and spectral distribution. However, only the 0.6-μsec component is readily identifiable in the luminescence. A survey of luminescence bands in the NaBr crystal we used showed the presence of a weak emission band near 3.1 eV which decayed in 400 μsec, and another near 3.5 eV which decayed in 2.8 msec. It is not known whether these are intrinsic bands. Because of the infrared detector's response time, only the 30-μsec component of the absorption spectrum could be measured accurately below 1.1 eV. There was some indication of a component decaying faster than 2 μsec in the region below 0.8 eV. Although our data for NaBr and NaI are thus not as comprehensive as

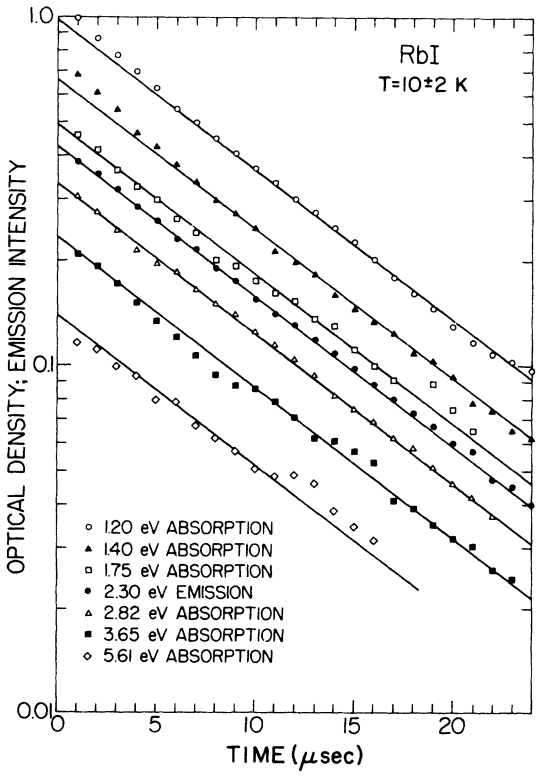

FIG. 5. Decay of absorption and triplet-exciton emission in RbI following a single pulse of 500-keV electrons. Some of the curves have been translated vertically for convenient display, so relative intensities are arbitrary.

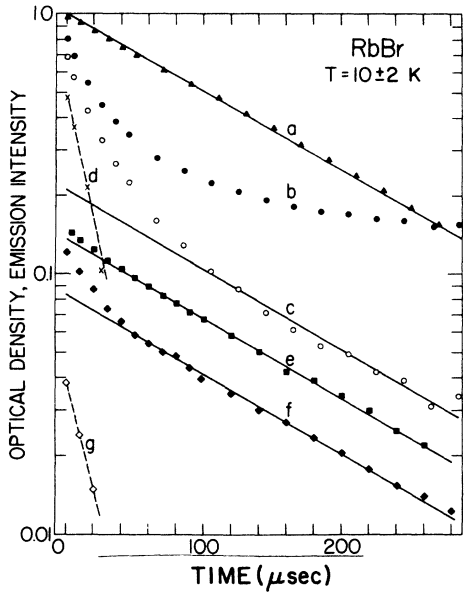

FIG. 6. Decay of absorption and triplet exciton emission in RbBr following a single pulse of 500-keV electrons: (a) 1.24-eV absorption (b) 1.82-eV absorption (as measured), (c) 1.82-eV absorption (minus stable component), (d) 1.82-eV absorption (fast component), (e) 2.10-eV luminescence, (f) 3.35-eV absorption (as measured), (g) 3.35-eV absorption (fast component).

those for the other crystals, we have nevertheless included them for completeness and to provide additional comparisons with our conclusions.

The optical density scales in Figs. 2–4 are normalized approximately to an excitation intensity of 2×10^{16} eV/cm^2 per electron pulse, with the optical path described earlier. Errors associated with the dosimetry and with fluctuations in the pulse energy make the normalization uncertain by about a factor of 2.

The transient absorption bands which do not overlap spectrally with strong color-center bands (e.g., F or H bands) show no significant dependence on whether the sample has been previously irradiated. However, the formation and decay of the color center bands themselves depends on the irradiation history of the sample. Thus to clarify the significance of color-center bands which appear in our data, we remark that peak-absorption strengths correspond to the first irradiation pulse on a new crystal; the one exception being NaCl, where we show the F formed on the fifth pulse. By designating a band as stable, we mean that it was observed approximately 3 min after the electron pulse, the crystal having spent the intervening time in darkness except for the single light flash used in the measurement process.

On the basis of the decay-time correspondence already noted, it is obviously reasonable to identify the spectra shown in solid lines in Figs. 2–4 as transitions originating in the lowest triplet state of the self-trapped exciton. Let $1/\tau$ be the probability for radiative decay of an excited state, and let $n(t)$ be the time-dependent population of the excited state. Then the intensity of luminescence emitted at time t is $I(t)\propto n(t)/\tau_R$. If light is absorbed in a transition from that same excited state to some higher state, the measured optical density $D(t)$ is proportional to the first-excited-state population, $D(t)\propto n(t)$. Thus the optical density and luminescence intensity are proportional in this case, related through the constant decay time τ_R. The *measured* reciprocal decay time $1/\tau$ can be closely approximated as the sum of $1/\tau_R$ and a nonradiative probability $1/\tau_N(T)$ which increases exponentially with temperature. Since $1/\tau_N$ enters the expressions for $I(t)$ and $D(t)$ only through the common factor $n(t)\propto e^{-(t/\tau_R+t/\tau_N)}$, the correspondence between emission and absorption decay times should persist through the temperature of thermal quenching if the same state originates both transitions. This relationship is verified for KBr in Fig. 7, which shows the experimentally observed temperature dependences of τ for luminescence and absorption. Agreement was also observed in the other cases tested—NaCl, KCl, and RbBr—although the results in RbBr were complicated by the appearance of additional components at higher temperatures.

For KCl and RbCl thermal quenching occurs at a particularly low temperature; at 12 K, τ has decreased by roughly 50% in both crystals. We ob-

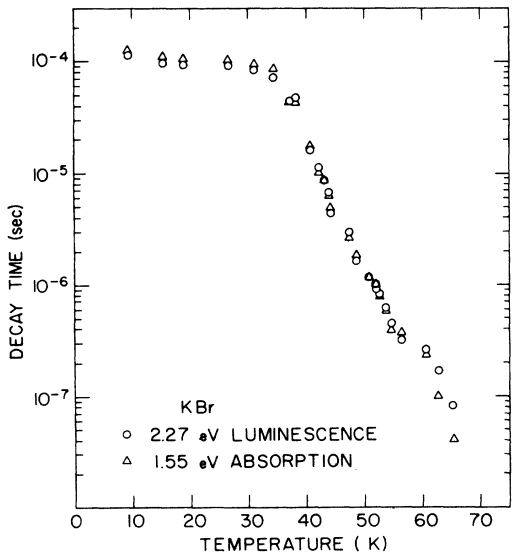

FIG. 7. Temperature dependence of the decay time for the triplet exciton luminescence and the 1.55-eV absorption in KBr.

served that when the pulse energy density was increased above a threshold near 10^{17} eV/cm^2, the decays became nonexponential and the nominal decay times of both absorption and emission in RbCl and KCl decreased by as much as two orders of magnitude. Below the threshold, the normal decay times were observed, except for a small persistent effect in RbCl. Since this behavior could not be produced in the materials with higher quench temperatures, we attributed it to momentary heating above 12 K in the electron penetration layer. By employing energy densities less than 10^{17} eV/cm^2, we could thus be certain that the temperature of any particular sample remained below about 12 K.

The possibility that the high electric fields arising from the negative charge deposited in the crystal could affect either τ_R or τ_N was also considered. However, at electron pulse energy densities below 10^{17} eV/cm^2 the decay of the luminescence is indistinguishable from that excited by a similar pulse of x rays, for which the effective energy density is lower by more than two orders of magnitude. This indicates that neither charging effects nor temperature excursions have had a significant influence on the data.

DISCUSSION

From the data discussed in the preceding section it is clear that we are observing transient absorption originating in the lowest triplet states of the STE. We can describe most of the features of these spectra in terms of a simplified model which assumes axial symmetry and which neglects the zero-field splittings of the triplet states. These splittings, which range from 3.3 μeV for KCl[13] to 690 μeV for KI,[14] are much smaller than the widths of the optical bands. Our approximate point group is thus $D_{\infty h}$, that of a homonuclear diatomic molecule. Beginning with the self-trapped hole or X_2^- molecular ion alone, the ground electronic configuration is

$$\cdots(\sigma_g np)^2(\pi_u np)^4(\pi_g np)^4(\sigma_u np) \equiv A \quad , \tag{1}$$

where n is the principal quantum number of the halogen valence shell. The hole orbital is σ_u, that is, p-like with respect to the center of symmetry.

Regarding the excited electron, it is clear that a more extensive orbital is required, particularly for the lowest triplet states for which one expects substantial amplitude on at least the ten nearest-neighbor alkali ions surrounding the X_2^-.[4,15,16] Furthermore, it is reasonable to expect the lowest excited electron orbital to be of over-all σ_g character, or s-like,[3] and this choice has proved consistent with all available data concerning the emission bands under consideration. We represent the lowest electron orbital schematically as $1s\sigma_g$, the $1s$ referring to the approximate symmetry of the envelope function outside the X_2^- core. The lowest triplet state is thus determined to be

$$A1s\sigma_g,\ ^3\Sigma_u^+ \ . \tag{2}$$

This is the initial state for the transitions to be described.

We first consider the broad absorption bands in the 2.7–4.0-eV range in Figs. 2 – 4 . In most crystals a single band is dominant, and it resembles in both location and shape the principal absorption band of the self-trapped hole or V_k center.[17] Since the core of the STE is, in fact, a perturbed X_2^- center, these transitions are identified as

$$D1s\sigma_g,\ ^3\Sigma_g^+ - A1s\sigma_g,\ ^3\Sigma_u^+ \ , \tag{3}$$

the excited configuration being

$$\cdots(\sigma_g np)(\pi_u np)^4(\pi_g np)^4(\sigma_u np)^2(1s\sigma_g) \equiv D1s\sigma_g \ . \tag{4}$$

There are additional configurations similar to Eq. (4) in which the hole is excited to $\pi_g np$ and $\pi_u np$ shells. The corresponding hole configurations are designated B and C, respectively. Transitions terminating in C are parity forbidden. However, absorption bands terminating in configuration B are observed for the stable X_2^- center; they are extremely weak in the chlorides, but in iodides they become comparable in intensity to those involving configuration D. The transient spectra over the ranges 1.6–3.8 eV in RbI and KI and 1.2–3.4 eV in NaI are, in fact, sufficiently similar to the corresponding X_2^- spectra[2] to suggest that the transition

$$B1s\sigma_g,\ ^3\Pi_g - A1s\sigma_g,\ ^3\Sigma_u^+ \tag{5}$$

is the probable origin of the 1.75-, 1.67-, and 1.40-eV peaks in RbI, KI, and NaI (Fig. 4). This transition is also a possible source for the weak band at 1.6 eV in NaBr. The present evidence on this assignment cannot be regarded as conclusive, however.

Having exhausted the hole configurations anticipated in this range of energy, we now turn to transitions involving the electron. Ignoring NaBr and NaI for the moment, each spectrum is seen to be characterized by a moderately sharp edge in the near infrared, one or more distinct peaks, and a gradual decline toward higher energy. These features are most readily interpreted in terms of Rydberg sequences terminating at the conduction band, analogous to the F and K bands arising from F centers.[18] The appropriate sequences are

$$Anp\sigma_u,^3\Sigma_g^+ - A1s\sigma_g,\ ^3\Sigma_u^+ \ , \tag{6}$$

$$Anp\pi_u,\ ^3\Pi_g - A1s\sigma_g,\ ^3\Sigma_u^+ \ . \tag{7}$$

where $n \geq 2$. Both converge to the same continuum. Although the exact shapes of the spectra these se-

quences should produce cannot be predicted, an edge at $n=2$ and a more gradual decline toward higher energy is the behavior one would generally expect.

This line of argument can be carried further, in that the doublet structures evident in KCl, RbCl, KBr, RbBr, and RbI can readily be ascribed to the $n=2$ components of the two sequences (6) and (7), with (6) accounting for the lower-energy peak. That is, the doublet corresponds to p-like electron orbitals oriented parallel and perpendicular to the molecular axis. The two peaks generally appear to be of comparable strength, a factor which weighs against their being the $n=2$ and 3 terms of either sequence alone. In the cases of NaCl and KI the doublet is presumably unresolved because of small separation and large broadening.

An interesting correlation becomes evident when one compares these STE bands with the absorption bands of related stable color centers. Let us consider the variations of band peak energies from crystal to crystal. For this purpose we plot peak energies versus the nearest-neighbor distance $\frac{1}{2}a$ in Fig. 8. As appropriate to these comparisons, the V_k or X_2^- band[17] and F band energies[18] are included and, in addition, the M band.[18] The latter band is the lowest-energy transition of the M center, a nearest-neighbor pair of F centers. The M center is electrically neutral and possesses the same point symmetry as the STE. In Fig. 8 the principal STE absorption peaks are represented by solid circles and prominent subsidiary peaks by open circles.

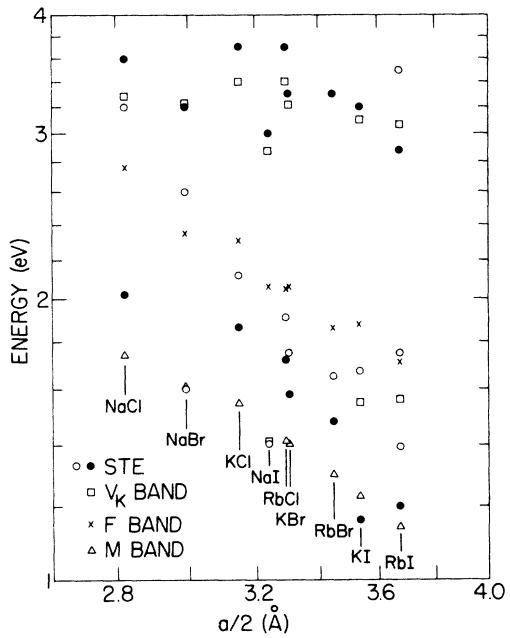

FIG. 8. Dependence on lattice parameter a of the peak energies of STE absorption bands and of absorption bands for stable F, M and V_k centers.

In the region around 3 eV the V_k and STE bands are seen to correlate rather well. Little, if any, systematic change with lattice parameter is evident, as might be expected for transitions involving orbitals localized in a molecular subunit such as an X_2^-. By contrast, the lower-energy STE bands show a distinct variation with $\frac{1}{2}a$ which parallels the variation evident in the F and M bands. These bands can be characterized by the well-known Mollwo-Ivey relationship[18] $E=Aa^{-m}$, where E is the peak energy and A and m are constants for a given center. The value $m\approx 2$ obtains for F and M centers. For the present purposes this relationship is considered simply as an empirical rule for electron centers, although there is some theoretical basis for it.[19] One sees from Fig. 8 that except for NaBr and NaI, the prominent lower energy STE bands conform roughly with this relationship, which fact provides additional circumstantial evidence that they are electron transitions. Indeed, there appears no plausible alternative to this assignment.

Other prominent transitions of the stable I_2^- center in the 1.4–1.6 eV range are included in Fig. 8, and the nearby open circles locate subsidiary STE transitions which we have suggested above are of similar origin, that is, due to transition (5). Several other subsidiary peaks from Figs. 2 – 4 are also included in Fig. 8.

Estimates of the optical binding energies E_i of the electron in the lowest triplet states can also be obtained from the spectra of Figs. 2 – 4. E_i is the limit of the Rydberg sequences (6) and (7), the ionic configuration being always that of the initial state. Consider first the relatively simple RbCl spectrum. Comparison with the F-center spectrum is of considerable help here, since the F and K bands are known to be transitions to a Rydberg-like sequence of p states terminating in the high-energy tail of the K band. In RbCl both photoconductivity measurements[20] and theoretical calculations[21] confirm this location for the band edge. Our estimated value for the STE ionization limit, $E_i=2.3\pm0.1$ eV, is chosen to be at the same energy with respect to the STE spectrum as is the band edge with respect to the F-center spectrum.

Similar estimates of E_i have been made from the other spectra in Figs. 2 – 4, making limited use of analogous color-center spectra as guides. These E_i, along with the peak energies of the doublet, are recorded in Table I. The reliability of E_i is clearly variable, this being evident from the ambiguity of the NaCl spectrum, for example.

Optical binding energies of *unrelaxed* excitons can be deduced from various fundamental optical spectra, the values being roughly 0.5 eV for the

TABLE I. Parameters of the triplet self-trapped exciton levels: Stokes shift in emission; measured transition energies corresponding to $n=2$ in Eqs. (6) and (7) of text; and estimated ionization limit corresponding to $n=\infty$ in Eqs. (6) and (7).

Material	Stokes shift (eV)	$n=2$ transitions (eV)		Ionization limit, E_i (eV)
RbCl	5.24	1.73	1.91	2.3 ± 0.1
KCl	5.44	1.87	2.12	2.6 ± 0.2
NaCl	4.58	2.02		2.8 ± 0.4
RbBr	4.50	1.48	1.65	2.2 ± 0.1
KBr	4.50	1.58	1.76	2.3 ± 0.3
NaBr	2.08			<1.1
RbI	3.40	1.20	1.38	1.7 ± 0.1
KI	2.46	1.15		1.7 ± 0.2
NaI	1.36			<1.2

iodides, 0.6 eV for the bromides, and 0.7 eV for the chlorides.[22] Despite the quantitative uncertainties inherent in our determinations of E_i, it is thus apparent that the optical binding energies for STE's are *greater* than those of *unrelaxed* excitons by factors of roughly 2–4. Some difference is to be expected, of course, since the ionic configurations which characterize the transitions are dissimilar. In the following we shall attempt to gain some qualitative insight into how these large E_i can come about.

As a first approximation one would attempt to account for the relaxation of the over-all system in terms of only one relaxation mode which is a superposition of displacements of a number of ions, that is, one configuration coordinate. This approximation has substantial utility when dealing with only two states. The solid curves of Fig. 9(a) depict the ground state and the lowest triplet in this manner, the configuration coordinate being designated r. The plane of this diagram can be considered to be a vertical section through the complete configuration space which intersects the absolute minima of the two states.

The onset of the ionization continuum, i.e., the common limit of sequences (6) and (7), must also be included in Fig. 9. Here use can be made of the V_k ground-state potential curve calculated by Jette *et al.*[23] However, it is important to realize that the minimum of the V_k potential will occur at an altogether different point in configuration space and thus in general will not lie in the plane of Fig. 9(a). We will assume that the vertical plane in configuration space which connects the minimum of this state with the minimum of the lowest-triplet STE is perpendicular to the plane of Fig. 9(a); i.e., that the system is describable by two orthogonal configuration coordinates. The second coordinate is labeled d. The dashed curve represents the V_k potential at and near its minimum point X', which should be regarded as displaced perpendicular to the plane of Fig. 9(a). The curve is sketched to have a shape similar to that of the theoretical curve for KCl. The only important parameter of this curve is its minimum energy $E(X')$. We can specify this, relative to the energy $E(Q)$ of a free electron-hole pair, on the basis of the measured activation energy for reorientation of the V_k center, which is 0.54 eV for KCl.[24] Following the calculation of Wood,[15] it is reasonable to estimate the energy difference $E(Q)-E(X')$ to be roughly 50% greater than the reorientation energy, that is, about 0.8 eV.

Since X' is the absolute minimum in the V_k configuration space, and Y is the absolute minimum in configuration space for the lowest-energy STE, the exciton binding energy must increase with relaxation along d; $E(X)-E(Y)\cong E(X')-E(Y')$. We can expect the difference in binding energy to be roughly halved between shifts of the ionized exciton (relaxed hole) and the lowest bound state. If the relaxation in coordinate d produces a shift from X to X' and from Y' to Y comparable to that for relaxation in r from Q to X' (≈ 0.8 eV), then the value $E_i=2.6$ eV in KCl is plausible, requiring only $E(X')-E(Y')=1$ eV. The latter value is comparable to the binding of an electron to an unrelaxed hole. KCl and NaCl represent the extreme cases of large E_i in Table I.

Figure 9(b) shows how the energies of the three states will depend upon d for a value of r fixed at the minima of the self-trapped states. The upper

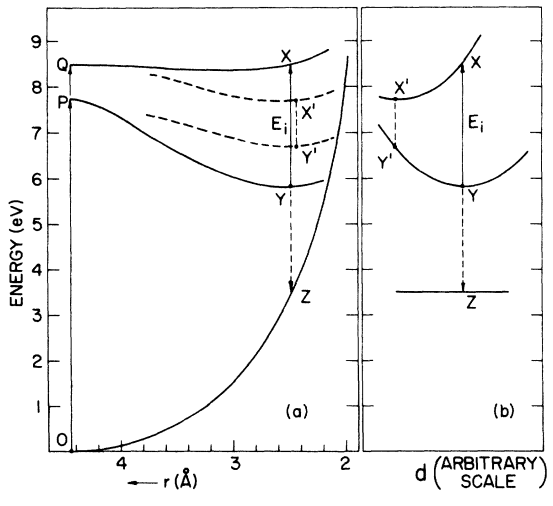

FIG. 9. Semiquantitative configuration coordinate diagrams for the STE in KCl. Coordinate r is the approximate internuclear spacing of the Cl_2^- core, and d represents schematically the displacements of all other ions. The determination of these curves is described in the text.

curves are seen to bear strong similarity to standard configuration curves for electron centers, e.g., those of Russell and Klick for the F center[25] and Hirai and Hashizume for the M center.[26] Curve $Y'Y$ would correspond to the ground state of the color center, and transitions $X \leftarrow Y$ and $X' \rightarrow Y'$ would correspond to optical absorption and emission, respectively.

It is a logical extension of the arguments presented thus far to speculate on the possibility that the environment which the electron experiences in the STE is in fact roughly equivalent to the environment an M-center electron experiences. Certainly the potential around the 10 nearest alkali ions and beyond is similar to that of the M center. In the M center the two electrons are kept apart by Coulomb repulsion, and it may well be that the average potential one M electron experiences due to the other electron is roughly equivalent to the average potential the electron in the STE experiences due to the net negative charge localized on the X_2^- core. Triplet-state lifetime data,[3] as well as recent EPR measurements,[13] seem to indicate that in crystals exhibiting large Stokes shifts, i.e., all of the present crystals except NaBr and NaI, the electron in the STE spends only a small fraction of its time on the X_2^- core.

We now return briefly to the spectra and consider the lower-energy region of the STE spectrum in comparison with that of the M center. Note first that with regard to the excited electron the orbitals proposed to describe the STE doublet, Eqs. (6) and (7), are the same as those which produce the M and M_F bands. Taking the M_F band to coincide approximately with the F, an assumption which should be valid in general, it is evident from Fig. 8 that the STE doublet falls generally between the M and M_F (or F) transitions for all crystals except NaBr and NaI. Except for the fact that the molecular field $(\sigma - \pi)$ splitting is substantially larger for the M center, there is actually fair *quantitative* resemblance between the spectra. In addition, our estimated E_i are comparable to those of M and F centers. The fact that we are here comparing singlet transitions of the M center with triplet transitions of the STE is of no consequence, since the relevant exchange energies for both are negligibly small on the scale of the optical spectra.[27,28]

On the basis of this model one can comment further on the physical significance of the coordinates r and d: It is clearly reasonable to associate r with the internuclear separation of the X_2^-; this separation, or more precisely the covalent bonding associated with it, is generally thought to be the principal contributor to the self-trapping energy, and the X_2^- internuclear repulsion accounts for almost all the ground-state energy variation. On the other hand, d would logically comprise the displacements of all other ions and thus would be identified with that (breathing) mode primarily responsible for the Stokes shift and broadening of the M-center spectra. Thus one would visualize Fig. 9(a) as describing the internal mode of the X_2^- and Fig. 9(b) as pertaining to an external mode. Obviously this separation of modes is a conceptual simplification which is valid only to some degree of approximation. For example, the two alkali ions nearest the center of the X_2^- must surely participate to some extent in the r relaxation.

We now draw attention to the fact that the scale of r in Fig. 9(a) is the actual internuclear separation of the Cl_2^- in the following sense: The ground potential curve has been calculated theoretically using standard procedures and Born-Mayer ionic potentials,[29] a relatively simple calculation which should be accurate to within about 10%. The energy of point Y was deduced as described above, and point Y was moved horizontally to that location giving the observed luminescent quantum $E(Y) - E(Z) = 2.32$ eV. The value of r at point Y (or, equivalently, X') is 2.48 Å, in satisfactory agreement with the V_k calculation of Jette *et al.*[23] when the latter is adjusted slightly to improve agreement with measurements of hyperfine splittings. This furnishes a useful consistency check which is, however, not very stringent. KCl has been used here as an example; however, diagrams similar to Fig. 9 have also been constructed for the other crystals,[29] and none is inconsistent with the model.

The remainders of the upper curves in Fig. 9 have been sketched to conform to the expected qualitative behavior. For Fig. 9(b) it is difficult to estimate the shape of the ground-state potential curve; it should vary relatively little and consequently has been shown as a horizontal line.

Consider now the case of the electron transitions, Eqs. (6) and (7), for NaBr and NaI. A straightforward extrapolation of the data of Fig. 8 would lead one to expect these transitions to appear in the 1.5–2.3-eV range for NaBr and the 1.3–2.0-eV range for NaI. There is STE absorption in these regions, but it shows little of the character of the electron transitions in other crystals. It seems more probable that at least most of the absorption given by the solid curves in Figs. 3 and 4 is caused by the hole transitions designated in Eqs. (3) and (5), as previously noted. Furthermore, in the context of our discussion involving Fig. 9, the relatively small Stokes shifts for NaBr and NaI, as shown in Table I, are not compatible with large E_i values.

It is most likely the electron transitions in NaBr and NaI occur at lower energies, below about 1 eV. The strong 30-μsec band which appears in the infrared region of the NaBr spectrum may have this origin. Although this lifetime component has not

been unambiguously identified with the intrinsic luminescence, the correspondence between the two components at shorter wavelength is difficult to explain otherwise. Multiple decay components occur generally in the iodide STE luminescence[14]; they arise from the marked differences in the character of the three triplet sublevels, A_u, B_{2u}, and B_{3u}. In fact, the small 3-μsec component seen in Fig. 4 for RbI arises in this way; it corresponds to a luminescence component from the B_{2u} and B_{3u} levels, while the stronger 11-μsec component originates in the A_u level.

In accord with the preceding discussion the estimated upper limits on E_t shown in Table I for NaBr and NaI depart substantially from those for the other crystals. It seems reasonable to conclude that KCl, RbCl, KBr, RbBr, and RbI represent the limit where the X_2^- core is largely uncoupled from the lattice; the electron and hole are somewhat independent of each other and behave like analogous perturbed color centers, M and V_k. Consequently the E_t are large, Stokes shifts are maximized, and luminescent lifetimes are long. At the other extreme are NaBr and NaI. For these crystals formation of the distinctive X_2^- core is still the driving force for self-trapping, but other aspects of the STE are perhaps better described in terms of a perturbation on the behavior of the free exciton rather than as analogs to perturbed color centers. KI and, to a lesser degree, NaCl might be regarded as falling somewhere between these two extremes. NaBr and NaI should still be characterizable in terms of configuration coordinate diagrams qualitatively similar to that of Fig. 9. Such diagrams have been derived and are consistent within the large uncertainties of E_t for these crystals.

Our analysis carries the clear implication that STE's in the RbCl category should produce a stronger perturbation on the nearby lattice than those at the NaI extreme. The relative locations of the perturbed exciton transitions above 5 eV in Fig. 4 confirm this to be the case. The shift of this transition with respect to the intrinsic exciton absorption is a measure of the perturbation and, as previously indicated,[5] these shifts are 0.12 eV for RbI, 0.14 eV for KI, but less than 0.05 eV for NaI.

We might remark, finally, that this behavior may be correlated with ion size considerations; that is, the farther apart the halide ions in the undisturbed lattice, the greater the relaxation in forming the X_2^-, and thus the more localized the hole and the more isolated the X_2^- from the electron. For the electron, the alkali ions are evidently a region of low potential relative to the X_2^- core, and for RbCl the relative size of the low-potential region is larger than, for example, for NaI.

ACKNOWLEDGMENTS

The authors acknowledge gratefully the contributions of Professor R. G. Fuller to investigations of transient self-trapped exciton absorption which led up to the work presently reported. We wish to thank Dr. M. H. Reilly and Professor W. B. Fowler for helpful discussions and Dr. V. H. Ritz for experimental advice.

[1]M. N. Kabler, Phys. Rev. 136, A1296 (1964); R. B. Murray and F. J. Keller, Phys. Rev. 137, A942 (1965).
[2]R. B. Murray and F. J. Keller, Phys. Rev. 153, 993 (1967).
[3]M. N. Kabler and D. A. Patterson, Phys. Rev. Lett. 19, 652 (1967).
[4]R. G. Fuller, R. T. Williams, and M. N. Kabler, Phys. Rev. Lett. 25, 446 (1970).
[5]R. T. Williams and M. N. Kabler, Solid State Commun. 10, 49 (1972).
[6]M. Hirai, Y. Kondo, T. Yoshinari, and M. Ueta, J. Phys. Soc. Jap. 30, 1071 (1971).
[7]Y. Kondo, M. Hirai, and M. Ueta, J. Phys. Soc. Jap. 33, 151 (1972).
[8]R. T. Williams, R. G. Fuller, M. N. Kabler, and V. H. Ritz, Rev. Sci. Instrum. 40, 1361 (1969).
[9]T. Karasawa and M. Hirai, J. Phys. Soc. Jap. 34, 276 (1973).
[10]The rise time given is a generalization from the limited observations that have been made in that time regime. Some of the color-center bands, especially, may have complex growth behaviors.
[11]M. P. Fontana, H. Blume, and W. J. VanSciver, Phys. Status Solidi 29, 159 (1968).
[12]D. Pooley and W. A. Runciman, J. Phys. C 3, 1815 (1970).
[13]M. J. Marrone, F. W. Patten, and M. N. Kabler, Phys. Rev. Lett. 31, 467 (1973).
[14]J. U. Fischbach, D. Frohlich, and M. N. Kabler, J. Lumin. 6, 29 (1973).
[15]R. F. Wood, Phys. Rev. 151, 629 (1966).
[16]I. M. Blair, D. Pooley, and D. Smith, J. Phys. C 5, 1537 (1972).
[17]For a review of hole centers including the V_k, see M. N. Kabler in *Point Defects in Solids* edited by J. H. Crawford, Jr. and L. M. Slifkin (Plenum, New York, 1972), Vol. 1, p. 327.
[18]W. B. Fowler, in *Physics of Color Centers*, edited by W. B. Fowler (Academic, New York, 1968).
[19]R. F. Wood, J. Phys. Chem. Solids 26, 615 (1965).
[20]G. Spinolo and D. Y. Smith, Phys. Rev. 140, A2117 (1965).
[21]D. Y. Smith and G. Spinolo, Phys. Rev. 140, A2121 (1965).
[22]For example, see D. Frohlich and B. Staginnus, Phys. Rev. Lett. 19, 496 (1967).
[23]A. N. Jette, T. L. Gilbert, and T. P. Das, Phys. Rev. 184, 884 (1969).

[24]R. D. Popp and R. B. Murray, J. Phys. Chem. Solids 33, 601 (1972).
[25]G. A. Russell and C. C. Klick, Phys. Rev. 101, 1473 (1956).
[26]M. Hirai and K. Hashizume, J. Phys. Soc. Jap. 24, 1059 (1968).
[27]M. N. Kabler, M. J. Marrone, and W. B. Fowler, in *Luminescence of Crystals, Molecules, and Solutions*, edited by F. Williams (Plenum, New York, 1973), p. 171.
[28]W. B. Fowler, M. J. Marrone, and M. N. Kabler, Phys. Rev. B 8, 5909 (1973).
[29]R. T. Williams, M. H. Reilly, and M. N. Dabler (unpublished).